

Fixing Two-Nucleon Weak-Axial Coupling $L_{1,A}$ From μ^-d Capture

Jiunn-Wei Chen,¹ Takashi Inoue,^{1,2} Xiangdong Ji,³ and Yingchuan Li³

¹*Department of Physics, National Taiwan University, Taipei, Taiwan 10617*

²*Department of Physics, Sophia University, Chiyoda-ku, Tokyo 102-8554, Japan*

³*Department of Physics, University of Maryland, College Park, Maryland 20742*

(Dated: September 21, 2018)

We calculate the muon capture rate on the deuteron to next-to-next-to-leading order in the pionless effective field theory. The result can be used to constrain the two-nucleon isovector axial coupling $L_{1,A}$ to ± 2 fm³ if the muon capture rate is measured to 2% level. From this, one can determine the neutrino-deuteron break up reactions and the pp -fusion cross section in the sun to a same level of accuracy.

The strong evidence of neutrino oscillations observed at the Sudbury Neutrino Observatory (SNO) [1] is based on detecting the ^8B solar neutrino flux through the following three reactions:

$$\begin{aligned} \nu_e + d &\rightarrow p + p + e^- & (\text{CC}), \\ \nu_x + d &\rightarrow p + n + \nu_x & (\text{NC}), \\ \nu_x + e^- &\rightarrow \nu_x + e^- & (\text{ES}). \end{aligned} \quad (1)$$

The charged current (CC) reaction involves only the electron neutrinos, while the neutral current (NC) reaction and elastic scattering (ES) involve all the active neutrinos ($x = e, \mu, \tau$). The ν_e and ν_x fluxes are found to be significantly different [1]. Further detailed measurements of the fluxes could sharpen the constraints to neutrino oscillation parameters and provide precision tests to the standard solar model [2]. However, while the ES cross section is known to high accuracy, the CC and NC cross sections have hadronic uncertainties. As shown by Butler, Chen and Kong [3], the dominant uncertainties in low energy CC and NC cross sections comes from the coupling of a two-body isovector axial current, $L_{1,A}$, in pionless effective field theory (EFT(\not{p})). The potential model results of Refs. [4] and [5] can be reproduced by different choices of $L_{1,A}$, indicating that the $\sim 5\%$ difference between the models comes from the different assumptions about the short-distance nuclear physics. There are other interesting weak reactions involving the same two-body current, for example, the pp and ppe^- fusion processes ($pp \rightarrow de^+\nu_e$, $ppe^- \rightarrow d\nu_e$) which power the sun [6, 7]. It is one of the great current interests to measure these neutrino fluxes to further test the standard solar model.

Recently much effort has been going into determining the effective two-body axial current interaction [8]. Butler, Chen, and Vogel attempted to fix $L_{1,A}$ from reactor antineutrino-deuteron breakup reactions, and they found $L_{1,A} = 3.6 \pm 5.5$ fm³ [8]. Chen, Heeger, and Robertson obtained $L_{1,A} = 4.0 \pm 6.3$ fm³ by using SNO's CC and NC data, calibrated by the ES events of SNO and Super-Kamiokande (SK) [9]. Schiavilla et al.'s idea [10] of using the tritium β decay rate to control the strength of the two-body current was adopted by Park et al. in their hybrid EFT calculation [11], and the pp

fusion rate was predicted with a small error. When compared with the EFT(\not{p}) calculation [7], their result yields $L_{1,A} = 4.2 \pm 2.5$ fm³.

In this paper we aim to make a high-precision determination of $L_{1,A}$ from the μ^-d capture process

$$\mu^- + d \rightarrow \nu_\mu + n + n, \quad (2)$$

by calculating the rate to next-to-next-to leading order (N²LO) in EFT(\not{p}). The μ^-d capture rate has been measured previously by different groups with rather different results $\Gamma^{\text{exp}} = 470 \pm 29$ s⁻¹ [12] and $\Gamma^{\text{exp}} = 409 \pm 40$ s⁻¹ [13]. A measurement of this rate with 1% precision is under investigation at PSI [14]. An earlier potential model calculation [15] gave $\Gamma = 397 \sim 400$ s⁻¹. More recently, the hybrid approach mentioned above gave $\Gamma = 386 \pm 5$ s⁻¹ [16].

A concern in applying EFT(\not{p}) to the μ^-d capture is that the energy transfer into the hadronic system might be too large to apply EFT(\not{p}). However, as shown in Ref. [16] and also in this calculation, the contribution to the total rate from high-energy neutrons is small, and it is possible to impose a neutron energy cut to isolate the low-energy ($\leq 10 - 20$ MeV) neutron events without significantly increasing the statistical errors [8, 14].

Effective field theory is useful when low and high energy scales in the problem are widely separated. For low-energy processes, short-distance physics can be taken into account by local operators in an effective lagrangian involving only low-energy degrees of freedom. For $\nu(\bar{\nu})-d$ scattering with neutrino energy below 20 MeV and μ^-d capture with small final-state neutron energy, the pion and other meson exchanges are not dynamical degrees of freedom, and their physics can be captured by contact interactions involving nucleons and the external currents. To make predictions with controlled precision, calculations are done with the perturbative expansion parameter $Q \equiv (1/a_{nn}^{(1S_0)}, \gamma, p)/\Lambda$, which is the ratio of light to heavy scales. The light scales include the inverse S-wave neutron-neutron scattering length $1/a_{nn}^{(1S_0)} = -10.6$ MeV in the 1S_0 channel, the deuteron binding momentum $\gamma = 45.7$ MeV in the 3S_1 channel, and typical nucleon momentum p in the system. The heavy scale Λ is

set by the pion mass m_π . This EFT(\not{p}) (see e.g. [17]) and its dibaryon version [18, 19, 20] have been applied successfully to many processes involving the deuteron, including electro-magnetic processes such as Compton scattering $\gamma d \rightarrow \gamma d$ [21, 22], $np \rightarrow d\gamma$ relevant to the big-bang nucleosynthesis [23, 24], weak processes such as νd reactions for SNO physics[3], the solar pp fusion process [6, 7], and parity violating observables [25]. For reviews on three-body systems, see [26].

The effective Lagrangian for the CC weak interaction is given by $\mathcal{L}^{CC} = -\sqrt{\omega_i} G_F V_{ud} l_\mu^\mu J_\mu^- / \sqrt{2} + \text{h.c.}$, where $G_F = 1.166 \times 10^{-5} \text{ GeV}^{-2}$ is the Fermi coupling constant and $\omega_i = 1.024$ takes into account the inner electroweak radiative correction [27]. $l_\mu^\mu = \bar{\nu}_\mu \gamma^\mu (1 - \gamma_5) \mu$ is the leptonic current. The quark current $J_\mu^- = V_\mu^- - A_\mu^- = (V_\mu^1 - A_\mu^1) - i(V_\mu^2 - A_\mu^2)$ contains both vector and axial-vector interactions, where the superscripts 1 and 2 are the isospin indices. At the scale relevant to nuclear physics, the quark current need be matched to a hadronic current which in general contains one-nucleon, two-nucleon, etc., operators.

Up to the order of our interest, the one-nucleon isovector vector and axial vector currents are

$$\begin{aligned} V_{(1)}^{0,a} &= N^\dagger \frac{\tau^a}{2} \left(1 + \frac{1}{6} \langle r^2 \rangle_c^{I=1} \bar{\nabla}^2 \right) N \\ V_{(1)}^{k,a} &= \frac{i}{2M_N} N^\dagger \bar{\nabla}_k \frac{\tau^a}{2} N - \frac{\mu^{(1)}}{M_N} \epsilon_{kij} N^\dagger \sigma_i \bar{\nabla}_j \frac{\tau^a}{2} N, \\ A_{(1)}^{0,a} &= \frac{ig_A}{2M_N} N^\dagger \vec{\sigma} \cdot \bar{\nabla} \frac{\tau^a}{2} N \\ &\quad - \frac{1}{4M_N^2} N^\dagger G_p \left(\bar{\nabla}^2 \right) \bar{\partial}_0 \vec{\sigma} \cdot \bar{\nabla} \frac{\tau^a}{2} N, \\ A_{(1)}^{k,a} &= g_A N^\dagger \sigma_k \frac{\tau^a}{2} \left(1 + \frac{1}{6} \langle r^2 \rangle_A^{I=1} \bar{\nabla}^2 \right) N \\ &\quad + \frac{1}{4M_N^2} N^\dagger G_p \left(\bar{\nabla}^2 \right) \bar{\nabla}_k \vec{\sigma} \cdot \bar{\nabla} \frac{\tau^a}{2} N, \end{aligned} \quad (3)$$

where $\bar{\nabla} = \bar{\nabla}_+ + \bar{\nabla}_-$, $\bar{\partial}_0 = \bar{\partial}_0_+ + \bar{\partial}_0_-$, and $\bar{\nabla}^\dagger = \bar{\nabla}_+ - \bar{\nabla}_-$. The superscript a is the isospin index, $\mu^{(1)} = (\mu_p - \mu_n)/2 = 2.353$, is the isovector magnetic moment. Isovector Dirac charge radius $\langle r^2 \rangle_c^{I=1} = \langle r^2 \rangle_c^p - \langle r^2 \rangle_c^n = 0.873 \text{ fm}^2$, and the isovector axial-charge radius $\langle r^2 \rangle_A^{I=1} \simeq 0.45 \text{ fm}^2$. We have neglected terms of order p^2/M_N^2 or even $\mu^{(1)} p^2/M_N^2$. The pseudoscalar form factor is, to a good approximation, dominated by the pion-pole $G_p(q^2) = \frac{4M_N^2 g_A}{M_\pi^2 - q^2}$ whose q^2 dependence will not be expanded because the momentum transfer $|\mathbf{q}|$ is of order muon mass M_μ with low energy final state neutrons. The G_p contribution to the axial current is counted of order Q .

The lowest dimensional two-nucleon isovector currents, in the dibaryon version of EFT(\not{p}), relevant to the $\mu^- d$

capture process are

$$\begin{aligned} V_{(2)}^{k,a} &= \frac{L_1^{db}}{M_N \sqrt{r^{(3S_1)} r_{nn}^{(1S_0)}}} \epsilon_{kij} t_i^\dagger \bar{\nabla}_j s_a + \text{h.c.}, \\ A_{(2)}^{k,a} &= \frac{L_{1,A}^{db}}{M_N \sqrt{r^{(3S_1)} r_{nn}^{(1S_0)}}} \left(t_k^\dagger s_a \right. \\ &\quad \left. + \frac{G_p}{4M_N^2 g_A} t_j^\dagger \bar{\nabla}_j \bar{\nabla}_k s_a \right) + \text{h.c.}, \end{aligned} \quad (4)$$

where t_i and s_a are dibaryon fields for the two-nucleon 3S_1 and 1S_0 states, respectively. The second term in $A_{(2)}^{k,a}$ is induced by the G_p term in the one-nucleon current. $r^{(3S_1)} = 1.764 \text{ fm}$ and $r_{nn}^{(1S_0)} = 2.8 \text{ fm}$ are the effective ranges in triplet and two-neutron singlet channels, respectively. L_1^{db} and $L_{1,A}^{db}$ are coupling constants in dibaryon formalism. The vector current is N²LO and its coupling $L_1^{db} = -4.08 \text{ fm}$ has been determined by the rate of $n + p \rightarrow d + \gamma$ near threshold. The axial current is NLO, and its coupling $L_{1,A}^{db}$ is proportional to the renormalization-scale- μ -independent $\tilde{L}_{1,A}$ in Ref. [3] as $L_{1,A}^{db} = \frac{M_N}{2\pi} \tilde{L}_{1,A}$, through which $L_{1,A}^{db}$ is related to the μ -dependent $L_{1,A}(\mu)$ in Ref. [3]. The numerical relation between $L_{1,A}^{db}$ and $L_{1,A}(\mu)$ is $L_{1,A}^{db} = L_{1,A}(\mu) = -13.8 + 0.28 L_{1,A}(M_\pi)$, where $L_{1,A}(M_\pi)$ is in units of fm^3 and has a natural size $\sim 6 \text{ fm}^3$.

The $\mu^- d$ atom has a ground state with a hyperfine structure, corresponding to the total angular momentum $F = 3/2$ and $F = 1/2$. The $\mu^- d$ capture process is known to take place almost uniquely from the doublet $F = 1/2$ state. The differential capture rate for muon and deuteron in their specific polarization states can be written in terms of leptonic tensor $l^{\mu\nu}$ and hadronic tensor $W_{\mu\nu}$ as

$$\frac{d\Gamma(S, \hat{\xi})}{dEd\Omega} = \frac{\omega_i G_F^2 |V_{ud}|^2 E |\psi(0)|^2}{32\pi^2 M_\mu (1 + \frac{M_\mu}{M_d})} l^{\mu\nu}(S) W_{\mu\nu}(\hat{\xi}), \quad (5)$$

where the $|\psi(0)|^2 = \frac{1}{\pi} \left(\alpha_{\text{em}} \frac{M_\mu M_d}{M_\mu + M_d} \right)^3$ is the $1S$ -state wave-function-at-origin-squared, E is the outgoing neutrino energy, and M_d is the mass of the deuteron.

The capture rate depends on the polarization vector of the muon S_μ and the deuteron polarization vector $\hat{\xi}$. The leptonic tensor is given by $l^{\mu\nu}(S) = 4(k^\mu k^\nu + k'^\mu k^\nu - k \cdot k' g^{\mu\nu} + i\epsilon^{\mu\nu\rho\sigma} k_\rho k'_\sigma) - 4M_\mu (S^\mu k'^\nu + k'^\mu S^\nu - k' \cdot S g^{\mu\nu} + i\epsilon^{\mu\nu\rho\sigma} S_\rho k'_\sigma)$, where $k = (M_\mu, \vec{0})$ and $k' = (E, \vec{k}')$, with $E = |\vec{k}'|$, are the four-momenta of initial muon and final ν_μ , respectively. The hadronic tensor is

$$W_{\mu\nu}(\hat{\xi}) = \frac{1}{\pi} \text{Im} \left[\int d^4 x e^{iqx} T \langle d | J_\mu^+(x) J_\nu^-(0) | d \rangle \right], \quad (6)$$

where $q_\mu = k_\mu - k'_\mu$, and $|d\rangle \equiv |d(P, \hat{\xi})\rangle$ is the deuteron state with momentum $P = (M_d, \vec{0})$ and polarization $\hat{\xi}$.

The diagrams contributing to $W_{\mu\nu}(\hat{\xi})$ up to N²LO are shown in Fig. 1. A straightforward calculation finds

$$\begin{aligned} \frac{d\Gamma}{dE} = & \frac{G_F^2 |V_{ud}|^2 E^2 |\psi(0)|^2}{2\pi(1 + \frac{M_\mu}{M_d})} \frac{1}{1 - \varepsilon\gamma r^{(3S_1)}} \left[\left(F_1 - \frac{F_2}{2} \right) \right. \\ & \left(3G_V^2 - 2(G_V - G_A)^2 - \varepsilon \frac{4g_A(1 - g_A)M_\mu E}{3(M_\pi^2 - q^2)} \right. \\ & \left. + \varepsilon\kappa^{(1)} \frac{8(1 - g_A)E}{3M_N} \right) + \left(F_1 - \frac{F_2}{6} + \frac{2}{3}F_{4a} \right) (9G_A^2 \\ & - \varepsilon \frac{6g_A^2 M_\mu E}{M_\pi^2 - q^2} + \varepsilon^2 \frac{g_A^2 E^4}{(M_\pi^2 - q^2)^2}) \\ & + (10F_1 - F_2 + 8F_{4b}) \frac{\varepsilon^2 \kappa^{(1)} E^2}{3M_N^2} \\ & + \left(F_1 - \frac{F_2}{6} + \frac{2}{3}F_{4c} \right) 12\varepsilon g_A \kappa^{(1)} \frac{E}{M_N} \\ & - (F_1 + F_{4c}) \frac{8\varepsilon^2 g_A \kappa^{(1)} E^3}{3M_N(M_\pi^2 - q^2)} \\ & \left. + F_5 \varepsilon^2 E \left(\frac{14}{3}g_A^2 + \frac{16}{3}g_A + 2 \right) \right] \quad (7) \end{aligned}$$

where $G_V = 1 + \varepsilon^2 \frac{1}{6} \langle r^2 \rangle_c^{I=1} q^2$ is the Dirac form factor, and $G_A = g_A(1 + \varepsilon^2 \frac{1}{6} \langle r^2 \rangle_c^{I=1} q^2)$ is the axial form factor. The ε is formally introduced to keep track of the Q expansion. After expanded in ε and truncated at ε^2 , the N²LO result is obtained by setting $\varepsilon = 1$. The functions $F_{1a,1b}$, F_2 , and $F_{3a,3b,3c}$ are from diagrams (a), (b), and (c), respectively, in Fig. 1

$$\begin{aligned} F_{1a} &= \frac{2M_N p \gamma}{\pi(M_N^2 \Delta_E^2 - p^2 E^2)} \\ F_{1b} &= \frac{\gamma}{\pi E^3} \left[\frac{2M_N E p \Delta_E}{M_N^2 \Delta_E^2 - p^2 E^2} + \ln \left(\frac{M_N \Delta_E - p E}{M_N \Delta_E + p E} \right) \right] \\ F_2 &= \frac{4\gamma}{\pi \Delta_E E} \tanh^{-1} \left(\frac{E p}{M_N \Delta_E} \right) \\ F_{3a} &= \frac{2\gamma M_N^2}{\pi^2 E^2} \text{Im} \left\{ G_1^2 A^{(1S_0)}(p) \right\} \\ F_{3b} &= \frac{2\gamma M_N^2}{\pi^2 E^2} \text{Im} \left\{ G_2^2 A^{(1S_0)}(p) \right\} \\ F_{3c} &= \frac{2\gamma M_N^2}{\pi^2 E^2} \text{Im} \left\{ G_1 G_2 A^{(1S_0)}(p) \right\}, \quad (8) \end{aligned}$$

with the re-scattering amplitude in the singlet channel as $A^{(1S_0)}(p) = -\frac{4\pi}{M_N} \left(\frac{1}{a_{nn}^{(1S_0)}} - \varepsilon \frac{1}{2} r_{nn}^{(1S_0)} p^2 + i p \right)^{-1}$, and functions $G_{1,2}$ are defined as $G_1 = \tan^{-1} \left(\frac{E}{2(\gamma - i p)} \right) + \varepsilon \frac{E}{4M_N g_A} L_{1,A}^{db}$ and $G_2 = \tan^{-1} \left(\frac{E}{2(\gamma - i p)} \right) + \varepsilon \frac{E}{4\mu^{(1)}} L_1^{db}$. The energy injection into the two-neutron system is $\Delta_E \equiv M_\mu - E - (M_n - M_p)$. The relative momentum between the two final-state neutrons is $2p$, with $p = \sqrt{M_N \Delta_E - \gamma^2 - E^2/4}$.

Power counting for the present calculation is rather tricky, and it would be misleading, for example, to just

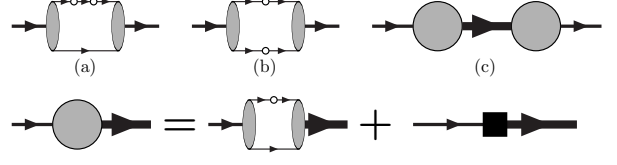


FIG. 1: Diagrams contributing to $W_{\mu\nu}(\hat{\xi})$ up to N²LO. The lines inside the loop are the nucleon propagators, and the thin and thick lines outside represent the triplet and singlet dibaryon fields, respectively. The small open circle represents the insertion of hadronic one-body current. In diagram (c), the large gray circle indicates the two possible hadronic current insertions shown in the second row where the dark square denotes the two-body current associated with $L_{1,A}$ and L_1 .

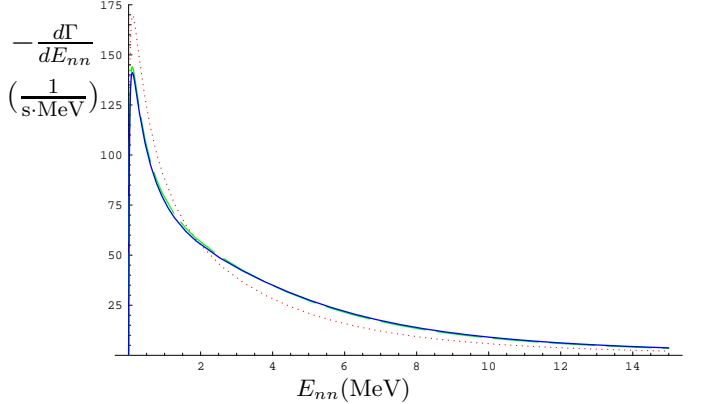


FIG. 2: (Color online) The differential capture rate $d\Gamma/dE_{nn}$ calculated using $L_{1,A} = 6 \text{ fm}^3$. The dotted line is the LO result. The dashed and solid lines, which sit on top of each other in this scale, are the NLO and N²LO results, respectively.

use the p/m_π to estimate the accuracy of the expansion. For example, it is well-known that in the nucleon-nucleon scattering, the effective theory without pion works rather well at the nucleon momentum on the order of 100 MeV, a value close to the pion mass. This can also be seen in the present calculation because the NLO result at large neutron momentum does not completely modify the leading order result, whereas the naive power counting would indicate otherwise. Fortunately, for muon capture, the most of the events occur when the neutron momentum is about half of the muon mass, that is, about 50 MeV.

In Fig. 2 we show the differential rate $d\Gamma/dE_{nn}$ in terms of the relative motion energy $E_{nn} = 2(\sqrt{M_N^2 + p^2} - M_N)$ of two final-state neutrons in the region where the EFT(\hat{f}) calculation is most reliable. It is clear from the figure that the differential rate in the energy region $E_{nn} \geq 10 \text{ MeV}$ is very small, and is negligible for $E_{nn} \geq 15 \text{ MeV}$. By comparing the results of LO, NLO, and N²LO, we find good convergence of the expansion.

In the case that a neutron energy cut can be imposed on experimental data [14], it is possible to define and measure the integrated capture rate up to a threshold

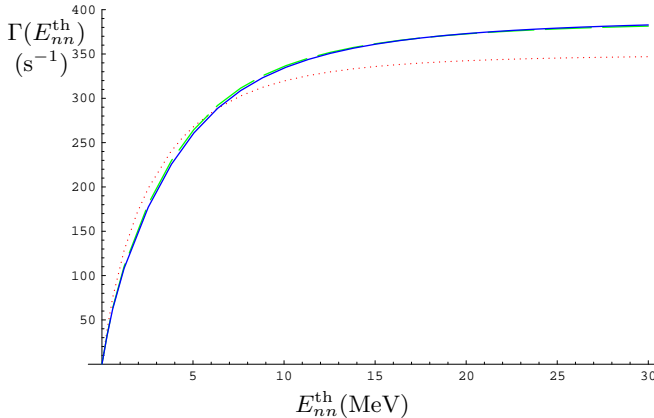


FIG. 3: (Color online) The integrated capture rate $\Gamma(E_{nn}^{\text{th}})$ calculated using $L_{1,A} = 6 \text{ fm}^3$ for the relative energy E_{nn}^{th} of the two neutrons up to 30 MeV. The description of the lines is the same as that in the caption of Fig. 2.

energy E_{nn}^{th}

$$\Gamma(E_{nn}^{\text{th}}) \equiv - \int_0^{E_{nn}^{\text{th}}} \frac{d\Gamma}{dE_{nn}} dE_{nn}. \quad (9)$$

The result up to 30 MeV is shown in Fig. 3. In the whole energy region, the NLO contribution is less than 10% of the LO contribution, while the N²LO contribution is less than 1%. This small size of N²LO contribution is accidental and does not happen for unpolarized and $F = 3/2$ rates. For example, the unpolarized rate has the expansion (for $L_{1,A} = 6 \text{ fm}^3$)

$$\Gamma_{\text{unpol.}} = \Gamma_{\text{unpol.}}^{\text{LO}} (1 + 5.3\% + 4.9\%), \quad (10)$$

where the NLO correction is abnormally small, and NNLO is of the normal size. A similar expansion is obtained for $L_{1,A} = -6 \text{ fm}^3$:

$$\Gamma_{\text{unpol.}} = \Gamma_{\text{unpol.}}^{\text{LO}} (1 + 10.9\% + 5.2\%) \quad (11)$$

which shows a nice convergence pattern. Based on this trend, we assign a 2-3% correction at NNNLO, corresponding to an error in $L_{1,A} \sim 2 \text{ fm}^3$. This is consistent with the naive estimation of 3% if the small expansion parameter is 1/3. A calculation shows the N³LO final state P-wave re-scattering contributes only $\sim 1\%$. Furthermore, the result is insensitive to the uncertainty in $a_{nn}^{(1S_0)}$. Choosing $L_{1,A} = 5.6 \text{ fm}^3$, the energy dependence of our result matches the previous hybrid calculation very well [16].

To extract $L_{1,A}$ from experimental data, it is useful to provide the dependence of the rate on $L_{1,A}$

$$\Gamma(E_{nn}^{\text{th}}) = a(E_{nn}^{\text{th}}) + b(E_{nn}^{\text{th}})L_{1,A}, \quad (12)$$

where $L_{1,A}$ is in unit of fm^3 . The energy-cut dependent functions $a(E_{nn}^{\text{th}})$ and $b(E_{nn}^{\text{th}})$ for a set of E_{nn}^{th} s are listed in the Table 1, from which we observe that, for the whole

range of E_{nn}^{th} , the size of $b(E_{nn}^{\text{th}})$ is about $1.3 \sim 1.5\%$ of the size of $a(E_{nn}^{\text{th}})$. This shows how an error in capture rate is translated into an uncertainty of $L_{1,A}$.

Table 1:
Coefficients functions $a(E_{nn}^{\text{th}})$ and $b(E_{nn}^{\text{th}})$ for specific values of two-neutron relative energy E_{nn}^{th} from the EFT(\not{p}) calculation.

$E_{nn}^{\text{th}}(\text{MeV})$	5.0	10.0	15.0	20.0
$a(E_{nn}^{\text{th}})(\text{s}^{-1})$	239.2	308.0	332.0	342.3
$b(E_{nn}^{\text{th}})(\text{s}^{-1}\text{fm}^{-3})$	3.3	4.2	4.7	4.9

In summary, we calculated the μ^-d capture rate using EFT(\not{p}) to N²LO. The major goal is to fix the two-nucleon isovector axial coupling constant $L_{1,A}$ from future precision experimental data. An experimental result on the integrated rate up to some neutron energy E_{nn}^{th} with a 2% error should be able to, through comparison with our calculation with theoretical error 2-3%, fix the $L_{1,A}$ with error $\pm 2.0 \text{ fm}^3$. This in turn allows us to determine the neutrino deuteron breakup cross section and the pp fusion rate in the sun to 2-3%.

This work was supported by the U. S. Department of Energy via grant DE-FG02-93ER-40762 and the NSC of Taiwan. We thank S. Ando, D.W. Hertzog, P. Kammel, K. Kubodera, and T.-S. Park for helpful discussions.

[1] Q.R. Ahmad *et al.*, Phys. Rev. Lett. **87**, 071301 (2001); **89**, 011301 (2002); **89**, 011302 (2002).

[2] J.N. Bahcall, A.M. Serenelli, and S. Basu, Astrophys. J. **621**, L85 (2005).

[3] M.N. Butler and J.W. Chen, Nucl. Phys. **A675**, 575 (2000); M.N. Butler, J.W. Chen, and X. Kong, Phys. Rev. **C63**, 035501 (2001).

[4] S. Ying, W.C. Haxton and E.M. Henley, Phys. Rev. **C45**, 1982 (1992); Phys. Rev. **D40**, 3211 (1989).

[5] S. Nakamura, T. Sato, V. Gudkov and K. Kubodera, Phys. Rev. **C63**, 034617 (2001).

[6] X. Kong and F. Ravndal, Nucl. Phys. **A656**, 421 (1999); **A665**, 137 (2000); Phys. Lett. **B470**, 1 (1999); Phys. Rev. **C64**, 044002 (2001).

[7] M. Butler and J.W. Chen, Phys. Lett. **B520**, 87 (2001).

[8] M. Butler, J.W. Chen, and P. Vogel, Phys. Lett. **B549**, 26 (2002).

[9] J.W. Chen, K.M. Heeger, and R.G.H. Robertson, Phys. Rev. **C67**, 025801 (2003).

[10] R. Schiavilla *et al.* Phys. Rev. **C58**, 1263 (1998).

[11] T.-S. Park *et al.*, nucl-th/0106025; nucl-th/0107012.

[12] G. Bardin *et al.*, Nucl. Phys. **A453** 591 (1986).

[13] M. Cargelli *et al.*, in: M. Morita, H. Ejiri, H. Ohtsubo, T. Sato (Eds.), Proceedings of the XXIII Yamada Conference on Nuclear Weak Processes and Nuclear Structure, Osaka, 1989, World Scientific, Singapore, P. 115 (1989).

[14] P. Kammel *et al.*, nucl-ex/0202011; nucl-ex/0304019.

[15] N. Tatara, Y. Kohyama, K. Kubodera, Phys. Rev. **C42**, 1694 (1990)

- [16] S. Ando, T.S. Park, K.Kubodera and F. Myhrer, Phys. Lett. **B533**, 25 (2002).
- [17] J.W. Chen, G. Rupak, and M.J. Savage, Nucl. Phys. **A653** 386 (1999)
- [18] D. B. Kaplan, Nucl. Phys. **B494**, 471 (1997).
- [19] S. R. Beane and M. J. Savage, Nucl. Phys. **A694**, 511, (2001).
- [20] S. Ando and C. H. Hyun, Phys. Rev. **C72**, 014008 (2005)
- [21] H.W.Griesshammer and G. Rupak, Phys. Lett. **B529**, 57 (2002).
- [22] J.W. Chen, X. Ji, and Y. Li, Phys. Lett. **B620**, 33 (2005); Phys. Rev. **C71**, 044321 (2005).
- [23] J.W. Chen and M.J. Savage, Phys. Rev. **C60**, 065205 (1999).
- [24] G. Rupak, Nucl. Phys. **A678**, 405 (2000).
- [25] M.J. Savage, Nucl. Phys. **A695**, 365 (2001).
- [26] P. F. Bedaque and U. van Kolck, Ann. Rev. Nucl. Part. Sci. **52**, 339 (2002); E. Braaten and H.-W. Hammer, cond-mat/0410417.
- [27] A. Sirlin, Rev. Mod. Phys. **50**, 573 (1978).